第 35 卷第 9 期
2019 年 9 月

无 机 化 学 学 报
CHINESE JOURNAL OF INORGANIC CHEMISTRY

Vol.35 No.9
1705-1711

两个基于刚性线型三羧酸配体的镍(Ⅱ)配合物的合成

邹训重[1] 吴 疆[2] 顾金忠*,[3] 赵 娜[1] 冯安生[1] 黎 彧*,[1]

([1]广东轻工职业技术学院,广东省特种建筑材料及其绿色制备工程技术研究中心/佛山市特种功能性建筑材料及其绿色制备技术工程中心,广州 510300)

([2]青海民族大学药学院,青藏高原植物资源化学省级重点实验室,西宁 810007)

([3]兰州大学化学化工学院,兰州 730000)

摘要:采用水热方法,选用刚性线型三羧酸配体(H_3L)和 2,2′-联吡啶(2,2′-bipy)与 $NiCl_2·6H_2O$ 分别在 120 和 160 ℃温度下反应,得到了一个具有零维双核镍结构的配合物$[Ni_2(\mu\text{-}HL)_2(2,2'\text{-}bipy)_2(H_2O)_4]·6H_2O$ (**1**)和一个一维链状配位聚合物$\{[Ni(\mu\text{-}HL)(2,2'\text{-}bipy)(H_2O)_2]·H_2O\}_n$ (**2**),并对其结构和磁性质进行了研究。结构分析结果表明 2 个配合物均属于三斜晶系,$P\bar{1}$ 空间群。配合物 **1** 具有零维双核镍结构,而且这些双核镍单元通过 O–H···O/N 氢键作用进一步形成了三维超分子框架,而配合物 **2** 具有一维链结构。2 个配合物的结构差异可能是由于水热反应温度不同造成的。研究表明,配合物 **2** 中相邻镍离子间存在反铁磁相互作用。

关键词:配位聚合物;氢键;三羧酸配体;磁性

中图分类号:O614.81+3 **文献标识码**:A **文章编号**:1001-4861(2019)09-1705-07

DOI:10.11862/CJIC.2019.190

Syntheses of Two Nickel(Ⅱ) Coordination Compounds Based on a Rigid Linear Tricarboxylic Acid

ZOU Xun-Zhong[1] WU Jiang[2] GU Jin-Zhong*,[3] ZHAO Na[1] FENG An-Sheng[1] LI Yu*,[1]

([1]*Guangdong Research Center for Special Building Materials and Its Green Preparation Technology/ Foshan Research Center for Special Functional Building Materials and Its Green Preparation Technology, Guangdong Industry Polytechnic, Guangzhou* 510300, *China*)

([2]*Key Laboratory for Tibet Plateau Phytochemistry of Qinghai Province, School of Pharmacy, Qinghai University for Nationalities, Xining* 810007, *China*)

([3]*College of Chemistry and Chemical Engineering, Lanzhou University, Lanzhou* 730000, *China*)

Abstract: Zero dimensional dinuclear nickel(Ⅱ) coordination compound and 1D chain nickel(Ⅱ) coordination polymer, namely $[Ni_2(\mu\text{-}HL)_2(2,2'\text{-}bipy)_2(H_2O)_4]·6H_2O$ (**1**) and $\{[Ni(\mu\text{-}HL)(2,2'\text{-}bipy)(H_2O)_2]·H_2O\}_n$ (**2**), have been constructed hydrothermally using 2,5-di(4-carboxylphenyl)nicotinic acid (H_3L), 2,2′-bipyridine (2,2′-bipy), and nickel chloride at 120 or 160 ℃, respectively. Single-crystal X-ray diffraction analyses revealed that both complexes crystallize in the triclinic system, space group $P\bar{1}$. Complex **1** discloses a discrete dimer structure, which is assembled to a 3D supramolecular framework through O–H ··· O/N hydrogen bond. Complex **2** has a chain structure. Structural differences between compounds **1** and **2** may be attributed to the different hydrothermal reaction temperature. Magnetic studies for complex **2** demonstrate an antiferromagnetic coupling between the adjacent Ni(Ⅱ) centers. CCDC: 1909474, **1**; 1909475, **2**.

Keywords: coordination polymer; hydrogen bonding; tricarboxylic acid; magnetic properties

收稿日期:2019-04-15。收修改稿日期:2019-05-25。

广东省高等职业院校珠江学者岗位计划资助项目(2015,2018),广东省自然科学基金(No.2016A030313761),广东轻院珠江学者人才类项目(No.RC2015-001),生物无机与合成化学教育部重点实验室开放基金(2016),广东省高校创新团队项目(No.2017GKCXTD001),广州市科技计划项目(No.201904010381),国家自然科学基金(No.21701032)和青海省科技计划项目(No.2018-ZJ-919)资助。

*通信联系人。E-mail:gujzh@lzu.edu.cn,liyuletter@163.com

0 Introduction

In recent years, the design and hydrothermal syntheses of functional coordination polymers have attracted tremendous attention owing to their fascinating architectures and topologies, as well as potential applications in catalysis, magnetism, luminescence and gas absorption[1-10]. Even after years of comprehensive study, it is difficult to predict the structures of coordination polymers, because a lot of factors influence the construction of complexes, such as the structural features of organic ligands, the coordination requirements of metal ions, solvent systems, temperatures, and pH values[11-17].

In this regard, various types of aromatic polycarboxylic acids have been proved to be versatile and efficient candidates for constructing diverse coordination polymers due to their rich coordination chemistry, tunable degree of deprotonation, and ability to act as H-bond acceptors and donors[3,13,17-20].

In order to extend our research in this field, we chose a rigid linear tricarboxylic acid ligand, 2,5-di(4-carboxylphenyl)nicotinic acid (H_3L), to construct novel coordination compounds. The ligand possesses the following features: (1) it contains a pyridyl and two phenyl rings with structural flexibility and conformation, and rotation of the C-C single bond between pyridyl and phenyl rings could form numbers of coordination geometries of metal ions; (2) it has seven potential coordination sites, one N atom from pyridyl ring and six O atoms of three carboxylate groups, which is beneficial to construct coordination polymers with interesting structures by its rich coordination modes; (3) it can act as hydrogen-bond acceptor as well as donor, depending upon the degree of deprotonation.

Taking into account these factors, we herein report the syntheses, crystal structures, and magnetic properties of two Ni (Ⅱ) coordination compounds constructed from H_3L.

1 Experimental

1.1 Reagents and physical measurements

All chemicals and solvents were of AR grade and used without further purification. Carbon, hydrogen and nitrogen were determined using an Elementar Vario EL elemental analyzer. IR spectra were recorded using KBr pellets and a Bruker EQUINOX 55 spectrometer. Thermogravimetric analysis (TGA) data were collected on a LINSEIS STA PT1600 thermal analyzer with a heating rate of 10 ℃·min^{-1}. Magnetic susceptibility data were collected in the 2 ~300 K temperature range with a Quantum Design SQUID Magnetometer MPMS XL-7 with a field of 0.1 T. A correction was made for the diamagnetic contribution prior to data analysis.

1.2 Synthesis of $[Ni_2(\mu\text{-HL})_2(2,2'\text{-bipy})_2(H_2O)_4]\cdot 6H_2O$ (1)

A mixture of $NiCl_2\cdot 6H_2O$ (0.024 g, 0.10 mmol), H_3L (0.036 g, 0.10 mmol), 2,2′-bipy (0.016 g, 0.1 mmol), NaOH (0.012 g, 0.20 mmol), and H_2O (8 mL) was stirred at room temperature for 15 min, and then sealed in a 25 mL Teflon-lined stainless steel vessel, and heated at 120 ℃ for 3 days, followed by cooling to room temperature at a rate of 10 ℃·h^{-1}. Blue block-shaped crystals of **1** were isolated manually, and washed with distilled water. Yield: 60% (based on H_3L). Anal. Calcd. for $C_{60}H_{58}Ni_2N_6O_{22}$ (%): C 54.08, H 4.39, N 6.31; Found(%): C 54.37, H 4.36, N 6.33. IR (KBr, cm^{-1}): 3 451m, 3 277m, 1 694m, 1 599s, 1 560s, 1 476w, 1 448m, 1 392s, 1 314w, 1 280w, 1 224w, 1 174w, 1 097w, 1 052w, 1 013w, 918w, 901w, 873w, 790w, 762m, 739w, 707w, 668w, 657w.

1.3 Synthesis of $\{[Ni(\mu\text{-HL})(2,2'\text{-bipy})(H_2O)_2]\cdot H_2O\}_n$ (2)

Synthesis of **2** was similar to **1** except using 160 ℃ instead of 120 ℃ as the temperature of hydrothermal reaction. Green block-shaped crystals of **2** were isolated manually, and washed with distilled water. Yield: 57% (based on H_3L). Anal. Calcd. for $C_{30}H_{25}NiN_3O_9$ (%): C 57.17, H 4.00, N 6.67; Found(%): C 56.92, H 3.98, N 6.69. IR (KBr, cm^{-1}): 3 339w, 3 033w, 1 677m, 1 604m, 1 560s, 1 521m, 1 476w, 1 431m, 1 386s, 1 319w, 1 287m, 1 192w, 1 153w, 1 125w, 1 103w, 1 058w, 1 008w, 968w, 918w, 857w, 806w, 778m, 734w, 711w, 678w, 650w. The complexes are insoluble in water and common organic solvents, such as methanol,

ethanol, acetone, and DMF.

1.4 Structure determinations

The data of two single crystals with dimensions of 0.25 mm×0.24 mm×0.22 mm (**1**) and 0.26 mm×0.23 mm×0.22 mm (**2**) were collected at 293(2) K on a Bruker SMART APEX Ⅱ CCD diffractometer with Mo $K\alpha$ radiation (λ=0.071 073 nm). The structures were solved by direct methods and refined by full matrix least-square on F^2 using the SHELXTL-2014 program[21]. All non-hydrogen atoms were refined anisotropically. All the hydrogen atoms were positioned geometrically and refined using a riding model. A summary of the crystallography data and structure refinements for **1** and **2** is given in Table 1. The selected bond lengths and angles for complexes **1** and **2** are listed in Table 2. Hydrogen bond parameters of complexes **1** and **2** are given in Table 3 and 4.

CCDC: 1909474, **1**; 1909475, **2**.

Table 1　Crystal data for complexes 1 and 2

Complex	1	2
Empirical formula	$C_{60}H_{58}Ni_2N_6O_{22}$	$C_{30}H_{25}NiN_3O_9$
Formula weight	1 332.54	630.24
Crystal system	Triclinic	Triclinic
Space group	$P\bar{1}$	$P\bar{1}$
a / nm	0.897 79(6)	0.697 47(5)
b / nm	1.223 20(8)	0.923 50(6)
c / nm	1.399 50(10)	2.118 55(15)
α / (°)	99.107(6)	91.484(5)
β / (°)	103.230(6)	90.892(6)
γ / (°)	94.417(5)	105.347(6)
V / nm^3	1.466 96(18)	1.315 13(16)
D_c / (g·cm^{-3})	1.508	1.592
Z	1	2
F(000)	692	652
θ range for data collection / (°)	3.397~25.049	3.415~25.048
Limiting indices	$-10 \leqslant h \leqslant 10, -14 \leqslant k \leqslant 14, -16 \leqslant l \leqslant 16$	$-8 \leqslant h \leqslant 7, -10 \leqslant k \leqslant 10, -24 \leqslant l \leqslant 25$
Reflection collected, unique (R_{int})	5 195, 4 254 (0.035 6)	4 644, 3 829 (0.032 7)
μ / mm^{-1}	0.729	0.803
Data, restraint, parameter	4 254, 0, 407	3 829, 0, 389
Goodness-of-fit on F^2	1.054	1.069
Final R indices [$I \geqslant 2\sigma(I)$] R_1, wR_2	0.046 3, 0.109 7	0.042 0, 0.086 8
R indices (all data) R_1, wR_2	0.058 8, 0.121 2	0.054 4, 0.095 7
Largest diff. peak and hole / (e·nm^{-3})	417 and −413	315 and −351

Table 2　Selected bond lengths (nm) and bond angles (°) for complexes 1 and 2

1					
Ni(1)-O(1)	0.206 6(2)	Ni(1)-O(4)A	0.207 8(2)	Ni(1)-O(7)	0.210 9(2)
Ni(1)-O(8)	0.208 6(2)	Ni(1)-N(2)	0.207 5(2)	Ni(1)-N(3)	0.205 9(2)
N(3)-Ni(1)-O(1)	177.71(9)	N(3)-Ni(1)-N(2)	79.30(10)	O(1)-Ni(1)-N(2)	100.39(9)
N(3)-Ni(1)-O(4)A	93.51(9)	O(1)-Ni(1)-O(4)A	86.78(8)	N(2)-Ni(1)-O(4)A	172.81(9)
N(3)-Ni(1)-O(8)	86.78(9)	O(1)-Ni(1)-O(8)	90.94(8)	N(2)-Ni(1)-O(8)	86.09(9)
O(4)A-Cu(1)-O(8)	93.46(8)	N(3)-Ni(1)-O(7)	91.25(9)	O(1)-Ni(1)-O(7)	91.02(8)
N(2)-Ni(1)-O(7)	90.72(9)	O(4)A-Ni(1)-O(7)	89.52(8)	O(8)-Ni(1)-O(7)	176.52(7)

Continued Table 2

2					
Ni(1)-O(2)	0.202 2(2)	Ni(1)-O(3)A	0.204 4(2)	Ni(1)-O(7)	0.214 1(2)
Ni(1)-O(8)	0.205 2(2)	Ni(1)-N(2)	0.206 1(2)	Ni(1)-N(3)	0.208 7(2)
O(2)-Ni(1)-O(3)A	92.61(8)	O(2)-Ni(1)-O(8)	87.09(8)	O(3)A-Ni(1)-O(8)	86.68(8)
O(2)-Ni(1)-N(2)	169.33(8)	O(3)A-Ni(1)-N(2)	97.63(8)	O(8)-Ni(1)-N(2)	90.50(9)
N(3)-Ni(1)-O(2)	91.08(8)	N(3)-Ni(1)-O(3)A	174.54(8)	N(3)-Ni(1)-O(8)	89.49(9)
N(3)-Ni(1)-N(2)	78.50(8)	O(2)-Ni(1)-O(7)	91.40(8)	O(3)A-Ni(1)-O(7)	89.42(8)
O(7)-Ni(1)-O(8)	175.75(7)	N(2)-Ni(1)-O(7)	91.69(9)	N(3)-Ni(1)-O(7)	94.52(8)

Symmetry codes: A: $-x+2$, $-y+1$, $-z+2$ for **1**; A: x, $y+1$, z for **2**.

Table 3 Hydrogen bond parameters for complex 1

D–H···A	*d*(D-H) / nm	*d*(H···A) / nm	*d*(D···A) / nm	∠DHA / (°)
O(6)–H(6)···O(9)A	0.082	0.175	0.256 0	169.6
O(7)–H(1W)···O(10)	0.082	0.205	0.281 2	154.3
O(7)–H(2W)···O(3)B	0.084	0.183	0.264 1	160.8
O(8)–H(3W)···O(2)	0.082	0.195	0.267 9	148.3
O(8)–H(4W)···N(1)C	0.085	0.196	0.278 3	164.8
O(9)–H(5W) ···O(2)D	0.085	0.192	0.276 8	179.7
O(9)–H(6W)···O(3)E	0.084	0.187	0.270 6	173.4
O(10)–H(7W)···O(5)F	0.086	0.201	0.282 6	160.1
O(10)–H(8W)···O(11)D	0.085	0.197	0.280 2	165.3
O(11)–H(9W)···O(10)	0.085	0.203	0.281 4	152.8
O(11)–H(10W)···O(1)	0.093	0.209	0.288 6	155.6

Symmetry codes: A: x, $y-1$, $z+1$; B: $-x+2$, $-y+1$, $-z+2$; C: x, $y+1$, z; D: $-x+1$, $-y+1$, $-z+1$; E: x, y, $z-1$; F: x, $y+1$, $z-1$.

Table 4 Hydrogen bond parameters for complex 2

D–H···A	*d*(D-H) / nm	*d*(H···A) / nm	*d*(D···A) / nm	∠DHA / (°)
O(6)–H(6)···O(9)A	0.082	0.181	0.263 1	176.5
O(7)–H(1W)···O(4)B	0.080	0.191	0.267 8	161.4
O(7)–H(2W)···O(1)	0.082	0.201	0.271 1	142.6
O(8)–H(3W) ···O(4)C	0.076	0.210	0.285 2	176.6
O(8)–H(4W)···O(5)D	0.082	0.194	0.274 2	163.8
O(9)–H(5W)···O(1)E	0.079	0.206	0.285 0	177.0
O(9)–H(6W)···O(2)F	0.090	0.203	0.292 7	174.2

Symmetry codes: A: x, $y+1$, $z+1$; B: x, $y+1$, z; C: $x+1$, $y+1$, z; D: $-x+1$, $-y+2$, $-z+2$; E: $-x$, $-y+1$, $-z+1$; F: $-x+1$, $-y+1$, $-z+1$.

2 Results and discussion

2.1 Description of the structure

2.1.1 $[Ni_2(\mu\text{-}HL)_2(2,2'\text{-bipy})_2(H_2O)_4]\cdot 6H_2O$ (**1**)

Single-crystal X-ray diffraction analysis reveals that complex **1** crystallizes in the triclinic space group $P\bar{1}$. Its asymmetric unit contains one crystallographically unique Ni(Ⅱ) ion, one μ-HL^{2-} block, one chelating 2,2′-bipy moiety, two H_2O ligands, and three lattice water molecules. As depicted in Fig.1, the six-coordinated Ni1 center is bound by two O atoms from two μ-HL^{2-} blocks, two O atoms from two H_2O ligands, and two N atoms from 2,2′-bipy moiety, thus resulting in an octahedral $\{NiN_2O_4\}$ environment. The lengths of the Ni-O bonds range from 0.206 6(2) to 0.210 9(2) nm, whereas the Ni-N distances vary from 0.205 9(2)

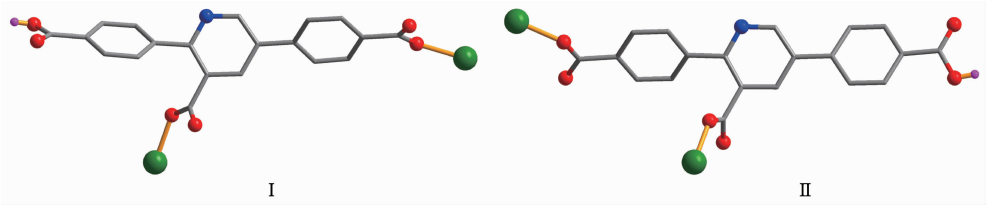

Scheme 1　Coordination modes of HL^{2-} ligands in complexes **1** and **2**

to 0.207 5(2) nm; these bonding parameters are comparable to those found in other reported Ni(Ⅱ) complexes[10,15]. In **1**, the HL^{2-} block behaves as a μ-spacer (mode Ⅰ, Scheme 1). Its nicotinate N donor remains uncoordinated while two COO^- groups are mono-dentate. The dihedral angles between pyridyl and phenyl rings in the HL^{2-} are 49.84° and 54.79°. The μ-HL^{2-} blocks connect two Ni1 ions to give a Ni_2 molecular unit having a Ni⋯Ni distance of 1.337 1(2) nm (Fig.2). These discrete Ni_2 units are assembled to a 3D supramolecular framework through O–H ⋯ O/N hydrogen bond (Fig.3 and Table 3).

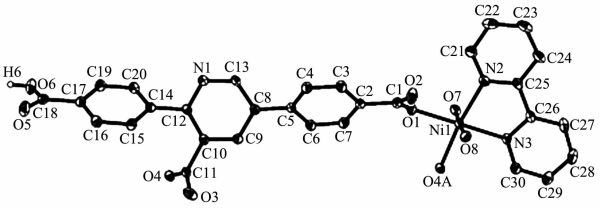

H atoms and lattice water molecules are omitted for clarity except H of COOH group; Symmetry code: A: $-x+2, -y+1, -z+2$

Fig.1　Asymmetric unit of complex **1** with 30% probability thermal ellipsoids

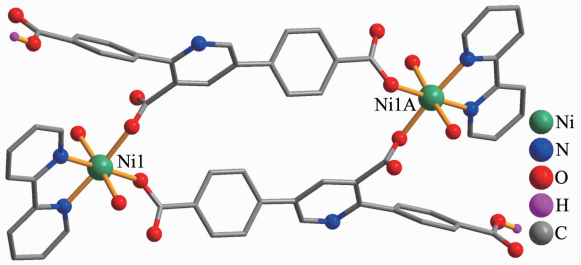

H atoms are omitted for clarity except the H of the COOH group; Symmetry code: A: $-x+2, -y+1, -z+2$

Fig.2　Dinuclear Ni(Ⅱ) unit of complex **1**

2.1.2　$\{[Ni(\mu\text{-}HL)(2,2'\text{-bipy})(H_2O)_2]\cdot H_2O\}_n$ (**2**)

The asymmetric unit of **2** consists of one Ni(Ⅱ) ion, one μ-HL^{2-} block, one 2,2′-bipy ligand, two coordinated and one lattice water molecules. As shown in Fig.4, six-coordinates Ni1 ion reveals a distorted

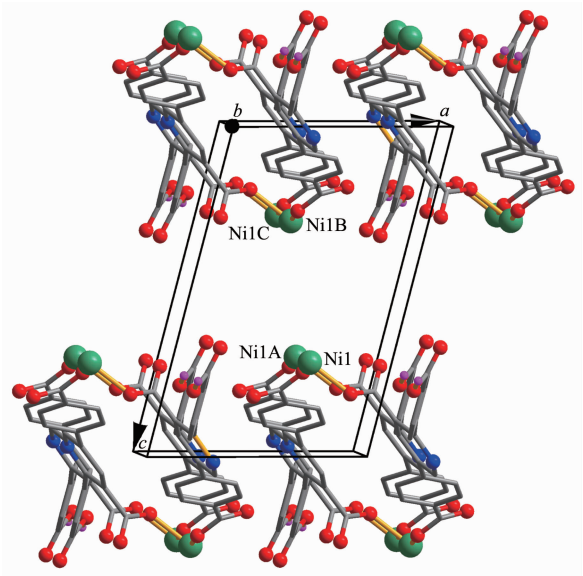

2,2′-bipy ligands and water molecules are omitted for clarity; Symmetry codes: A: $x, y-1, z$; B: $-x+1, -y+2, -z+1$; C: $-x+1, -y+1, -z+1$

Fig.3　Perspective of 3D supramolecular framework parallel to *ac* plane in **1**

octahedral $\{NiN_2O_4\}$ environment, filled by two carboxylate O atoms from two individual μ-HL^{2-} blocks, two O atoms from two H_2O ligands, and a pair of N atoms from 2,2′-bipy ligand. The Ni-O distances range from 0.202 2(2) to 0.214 1(2) nm, whereas the Ni-N distances vary from 0.206 1(2) to 0.208 7(2) nm; these bonding parameters are comparable to those observed in other Ni(Ⅱ) complexes[15,17-18]. In **2**, the HL^{2-} block acts as a μ-linker via monodentate COO^- groups (mode Ⅱ, Scheme 1), and the nicotinate N atom remains uncoordinated. In HL^{2-}, two dihedral angles between pyridyl and benzene rings are 19.52° and 42.02°. The HL^{2-} linkers connect the adjacent Nil centers to form a zigzag 1D chain with the Ni1 ⋯ Ni1 separation of 0.923 5(2) nm (Fig.5).

The nickel(Ⅱ) compounds **1** and **2** were prepared hydrothermally under similar reaction conditions,

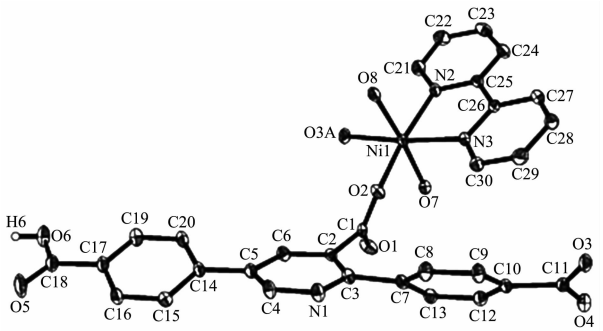

H atoms and lattice water molecules were omitted for clarity except H of COOH group; Symmetry code: A: x, y+1, z

Fig.4 Asymmetric unit of complex **2** with 30% probability thermal ellipsoids

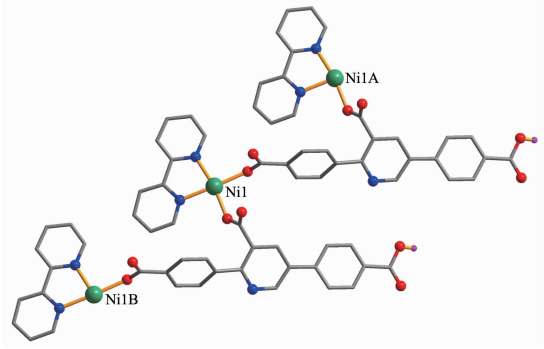

Symmetry codes: A: x, y+1, z; B: x, y−1, z

Fig.5 One dimensional chain viewed along a axis in **2**

except using different reaction temperatures (120 ℃ for **1** and 160 ℃ for **2**). The HL^{2-} ligands adopt different coordination modes at 120 and 160 ℃ (Scheme 1), which results in distinct structures[22-25].

2.2 TGA analysis

To determine the thermal stability of complexes **1** and **2**, their thermal behaviors were investigated under nitrogen atmosphere by thermogravimetric analysis (TGA). As shown in Fig.6, complex **1** lost its six

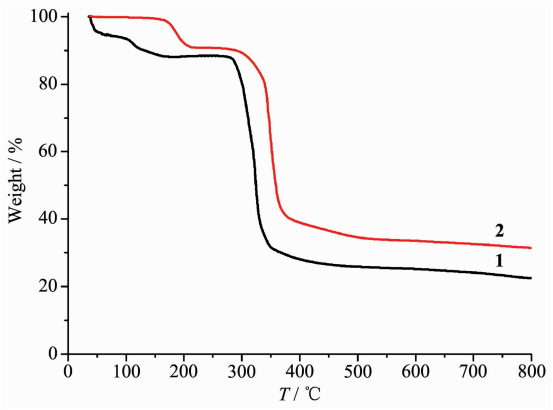

Fig.6 TGA curves of complexes **1** and **2**

lattice and four coordinated water molecules in the range of 36~178 ℃ (Obsd. 13.2%; Calcd. 13.5%), followed by the decomposition at 278 ℃. The TGA curve of **2** revealed that one lattice and two coordinated water molecules were released between 142 and 218 ℃ (Obsd. 8.9%; Calcd. 8.6%), and the dehydrated solid began to decompose at 271 ℃.

2.3 Magnetic properties

Variable-temperature magnetic susceptibility studies were carried out on powder sample of **2** in the 2~300 K temperature range. The $\chi_M T$ value at 300 K was 1.05 $cm^3 \cdot mol^{-1} \cdot K$, which is close to the expected one (1.00 $cm^3 \cdot mol^{-1} \cdot K$) for one magnetically isolated Ni(Ⅱ) ion (S=1, g=2.0). Upon cooling, the $\chi_M T$ value decreased very slowly from 1.05 $cm^3 \cdot mol^{-1} \cdot K$ at 300 K to 0.981 $cm^3 \cdot mol^{-1} \cdot K$ at 17 K, and then decreased steeply to 0.663 $cm^3 \cdot mol^{-1} \cdot K$ at 2 K. In the 2~300 K interval, the χ_M^{-1} vs T plot for **2** obeys the Curie-Weiss law with a Weiss contant θ of −5.23 K and a Curie constant C of 1.05 $cm^3 \cdot mol^{-1} \cdot K$. An empirical (Weng's) formula can be applied to analyze the 1D systems with S=1, using numerical procedures[26-27]:

$$\chi_M = \frac{N\beta^2 g^2}{kT} \frac{A}{B}$$

$$A = 2.0 + 0.019\ 4x + 0.777x^2$$

$$B = 3.0 + 4.346x + 3.232x^2 + 5.834x^2$$

with $x = |J|/kT$

Using this method, the best-fit parameters for **2** were obtained: g=2.08, J=−0.94 cm^{-1}, and R=7.7×10^{-5},

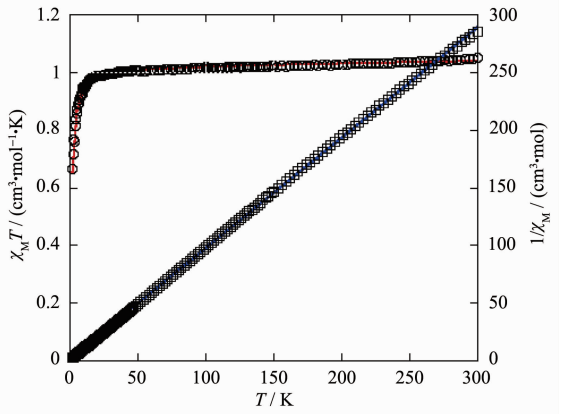

Red curve represents the best fit to the equations in the text; blue line shows the Curie-Weiss fitting

Fig.7 Temperature dependence of $\chi_M T$ (○) and $1/\chi_M$ (□) vs T for complex **2**

where $R=\sum(T_{obs}-T_{calc})^2/\sum(T_{obs})^2$. The J value of −0.94 cm^{-1} indicates that the coupling between the Ni(Ⅱ) centers is antiferromagnetic.

3 Conclusions

In summary, we have synthesized two Ni (Ⅱ) coordination compounds whose structures depend on the hydrothermal reaction temperature. This work demonstrates that the hydrothermal reaction temperature has a significant effect on the structures of the coordination compounds.

References:

[1] Zhao X, Wang Y X, Li D S, et al. *Adv. Mater.*, **2018**,**30**: 1705189

[2] Zhen X D, Lu T B. *CrystEngComm*, **2010**,**12**:324-336

[3] Lu W G, Su C Y, Lu T B, et al. *J. Am. Chem. Soc.*, **2006**, **128**:34-35

[4] Chen Q, Xue W, Lin J B, et al. *Chem. Eur. J.*, **2016**,**22**: 12088-12094

[5] Gu J Z, Wen M, Cai Y, et al. *Inorg. Chem.*, **2019**,**58**:2403-2412

[6] Kaurl R, Kim K H, Paul A K, et al. *J. Mater. Chem. A*, **2016**, 4:3991-4002

[7] Garai D A, Gude V, Biradha K. *Cryst. Growth Des.*, **2018**,**18**: 6070-6077

[8] Zhao D, Yue L, Zhang K, et al. *Inorg. Chem.*, **2018**,**57**:12596-12602

[9] Gu J Z, Wen M, Cai Y, et al. *Inorg. Chem.*, **2019**,**58**:5875-5885

[10]Gu J Z, Cai Y, Liang X X, et al. *CrystEngComm*, **2018**,**20**: 906-916

[11]Pal S, Pal T K, Bharadwaj P K. *CrystEngComm*, **2016**,**18**: 1825-1831

[12]Zhang L N, Zhang C, Zhang B, et al. *CrystEngComm*, **2015**, **17**:2837-2846

[13]Gu J Z, Gao Z Q, Tang Y. *Cryst. Growth Des.*, **2012**,**12**: 3312-3323

[14]Du M, Li C P, Liu C S, et al. *Coord. Chem. Soc.*, **2013**,**257**: 1282-1305

[15]Gu J Z, Cui Y H, Liang X X, et al. *Cryst. Growth Des.*, **2016**,**16**:4658-4670

[16]Dong Y B, Jiang Y Y, Li J, et al. *J. Am. Chem. Soc.*, **2007**, **129**:4520-4521

[17]Gu J Z, Liang X X, Cai Y, et al. *Dalton Trans.*, **2017**,**46**: 10908-10925

[18]Yue Q, Liu X, Guo W X, et al. *CrystEngComm*, **2018**,**20**: 4258-4267

[19]GU Wen-Jun(顾文君), GU Jin-Zhong(顾金忠). *Chinese J. Inorg. Chem.*(无机化学学报), **2017**,**33**(2):227-236

[20]ZHAO Su-Qin(赵素琴), GU Jin-Zhong(顾金忠). *Chinese J. Inorg. Chem.*(无机化学学报), **2016**,**32**(9):1611-1618

[21]Spek A L. *Acta Crystallogr. Sect. C: Struct. Chem.*, **2015**, **C71**:9-18

[22]Zhao N, Li Y, Gu J Z, et al. *Dalton Trans.*, **2019**,**48**:8361-8374

[23]Wan J, Cai S L, Zhang K, et al. *CrystEngComm*, **2016**,**18**: 5164-5176

[24]Chainok K, Ponjan N, Theppitak C, et al. *CrystEngComm*, **2018**,**20**:7446-7457

[25]Cai S L, Huang Y, Gao Y, et al. *Inorg. Chem. Commun.*, **2017**,**84**:10-14

[26]Kahn O. *Molecular Magnetism*. New York: VCH, **1993**.

[27]Weng C Y. *Thesis for the Doctorate of Carnegie Mellon University*. **1969**.